Full length article

Highly-branched poly(N-isopropyl acrylamide) functionalised with pendant Nile red and chain end vancomycin for the detection of Gram-positive bacteria

Thomas Swift [a], Maria Katsikogianni [a], Richard Hoskins [a], Pavintorn Teratarantorn [b], Ian Douglas [b], Sheila MacNeil [c], Stephen Rimmer [a,*]

[a] Polymer and Biomaterials Chemistry Laboratories, School of Chemistry and Biosciences, University of Bradford, Bradford BD7 1DP, UK
[b] School of Clinical Dentistry, University of Sheffield, Sheffield S10 2TA, UK
[c] Department of Materials Science and Engineering, Kroto Research Institute, University of Sheffield, Sheffield S3 7HQ, UK

ABSTRACT

This study shows how highly branched poly(N-isopropyl acrylamide) (HB-PNIPAM) with a chain pendant solvatochromic dye (Nile red) could provide a fluorescence signal, as end groups bind to bacteria and chain segments become desolvated, indicating the presence of bacteria. Vancomycin was attached to chain ends of HB-PNIPAM or as pendant groups on linear polymers each containing Nile red. Location of the dye was varied between placement in the core of the branched polymer coil or the outer domains. Both calorimetric and fluorescence data showed that branched polymers responded to binding of both the peptide target (D-Ala-D-Aa) and bacteria in a different manner than analogous linear polymers; binding and response was more extensive in the branched variant. The fluorescence data showed that only segments located in the outer domains of branched polymers responded to binding of Gram-positive bacteria with little response when linear analogous polymer or branched polymer with the dye in the inner core was exposed to *Staphylococcus aureus*.

© 2019 Acta Materialia Inc. Published by Elsevier Ltd. This is an open access article under the CC BY-NC-ND license (http://creativecommons.org/licenses/by-nc-nd/4.0/).

1. Introduction

As a new approach to developing cost-effective diagnostics, we recently described polymers that respond to either Gram-positive [1] or Gram-negative [2] bacteria in which binding events drive the polymer through a desolvation phase change; the coil-to-globule transition (T$_{c-g}$) [3]. T$_{c-g}$ is affected by: salt concentration; [4,5] the adsorption of surfactants [6]; and structural features such as charge [7] and chain architecture [8–12]. Using, Förster resonance energy transfer we were able to show that binding of a highly branched poly(N-isopropyl acrylamide) with vancomycin end groups (HB-PNIPAM-van) produced a desolvation transition on binding to *Staphylococcus aureus* [13]. Also, we provided evidence to show that equivalent linear polymer did not aggregate the bacteria despite being shown to bind the target D-alanyl-D-alanyl (D-Ala-D-Ala) [14–16]. Recently, Chen et al reported a bactericidal branched cationic polymer [17]. The central hypothesis developed on the action of these polymers has been that ligands placed at the chain ends of a highly branched polymer are available for binding

to cellular targets in both the open-coil solvated form and the desolvated globular form. We proposed that linear polymers with ligands pendant to the main chain would only bind to their targets in the open-solvated form because the desolvated structure would mask the binding interactions.

This implies an influence of chain end solvation on segment solvation and it is unlikely that these effects would be homogeneous throughout the coil. Chain end solvation would affect the end segments by increasing the osmotic potential of the outer domains of the highly branched coils. This principle is illustrated in Fig. 1, which shows a schematic of the domain structure with the inner (less swollen segments shown in black), the outer (more swollen segments) in blue and the end groups as spheres. Fig. 1B shows how binding of the end groups leads to deswelling and desolvation.

The use of these polymers as a diagnostic tool requires a method for reporting the phase change on binding of microbes. One way to do this would be to incorporate a solvatochromic dye, such as Nile red [18]. In this work a range of HB-PNIPAMs were synthesised using self-condensing reversible addition fragmentation transfer polymerization (SCVP-RAFT) [11] with the label located throughout the chain or in either the inner segments or outer segments of the highly branched structures. We also
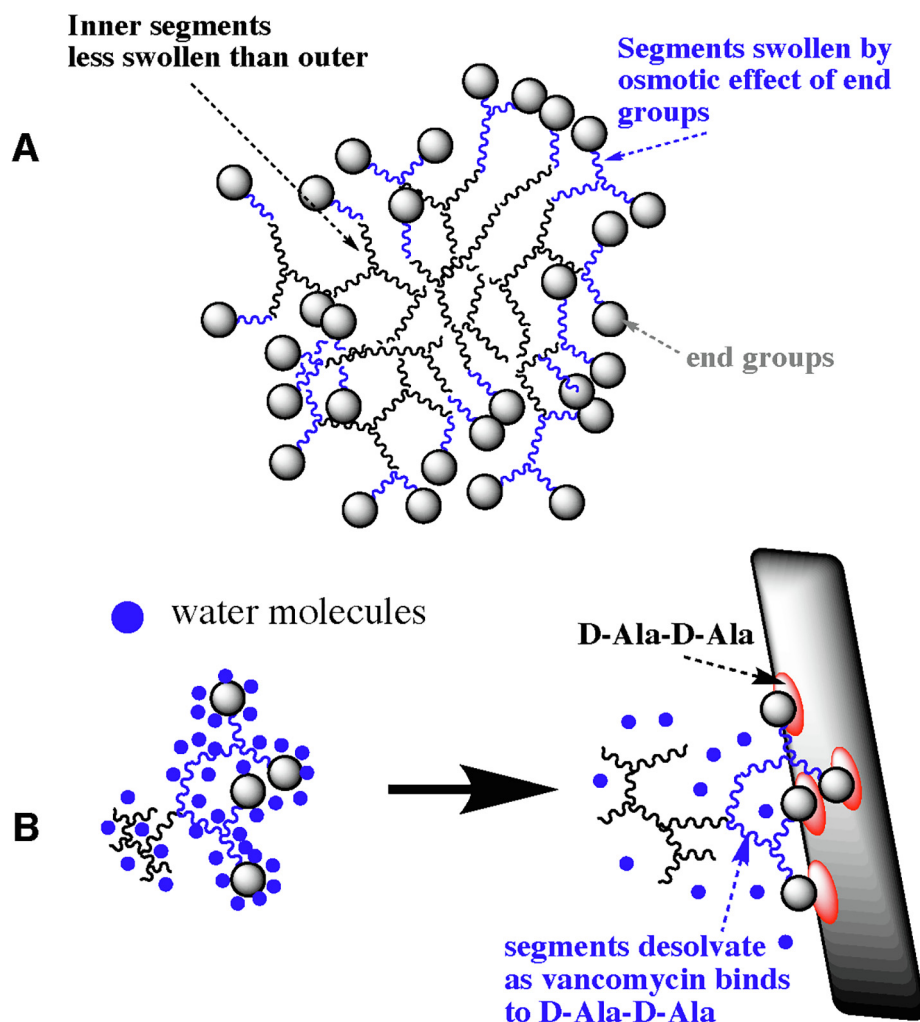
Fig. 1. (A) Schematic diagram of a highly branched polymer with chain end ligands; (B) diagram showing polymer segments binding and desolvation of the end segments.

prepared linear copolymers with Nile red pendant to the main chain. The SCVP-RAFT technique uses copolymerization with a "branching" monomer, such as 4-vinylbenzyl pyrrolecarbod-ithioate (**1**), containing both a polymerisable vinyl group and a dithioate ester that mediates the RAFT process. Nile red was incorporated by copolymerisation with Nile red acrylate (**2**) (see Scheme 1).

## 2. Materials and methods

2.1. Polymer synthesis

The following NIPAM copolymers were produced:

- **L-P0** Linear copolymer with pendant Nile red functionality.
- **L-P1** Linear copolymer with pendant Nile red and vancomycin functionality.
- **L-P2** Linear copolymer with vancomycin functionality (no Nile red).
- **HB-P3** Highly branched polymer with pendant Nile red throughout the polymer and vancomycin at the chain ends.
- **HB-P4** Highly branched polymer with no pendant Nile red throughout the polymer and no vancomycin at the chain end
- **HB-P5** Highly branched polymer with Nile red in inner chain segments and vancomycin at the chain ends.

- **HB-P6** Highly branched polymer with Nile red in outer branched segments and vancomycin at the chain ends.
- **HB-P7** Highly branched polymer with Nile red in outer linear segments and vancomycin at the chain ends.

Full synthetic routes for each material are shown in the supporting information. Each of these polymers were prepared in multiple steps (except for **L-P0**). To aid the reader **L** indicates a linear polymer and **HB** signifies a highly branched polymer. The first precursor of the branched polymer is identified through out by the subscript, p. **L-P1$_{COOH}$** is a copolymer of NIPAM, **2** and vinyl benzoic acid (**3**) and **L-P2$_{COOH}$** is a copolymer of NIPAM and **3**. The highly branched polymers (**HB-P3** to **HB-P7**) were produced using SCVP-RAFT, which allowed control over the architecture of the highly branched polymers and placement of the solvatochromic dye (Nile red). **HB-P4$_p$** is a branched polymer prepared without Nile red that serves as the precursor to polymers with outer segments containing Nile red. The carboxylic acid groups of **HB-P1$_{COOH}$** and **HB-P2$_{COOH}$** were then modified by reaction with vancomycin (pH 9) via the N-hydroxy succinimide (NHS) ester. The highly branched polymers were produced using modifications of our previously reported technique. The highly branched polymer with Nile red throughout the backbone, (**HB-P3$_p$**) was produced by copolymerizing NIPAM, **1** and **2**. The **HB-P5$_p$** polymer was then prepared in a second step copolymerization with NIPAM and **1**.
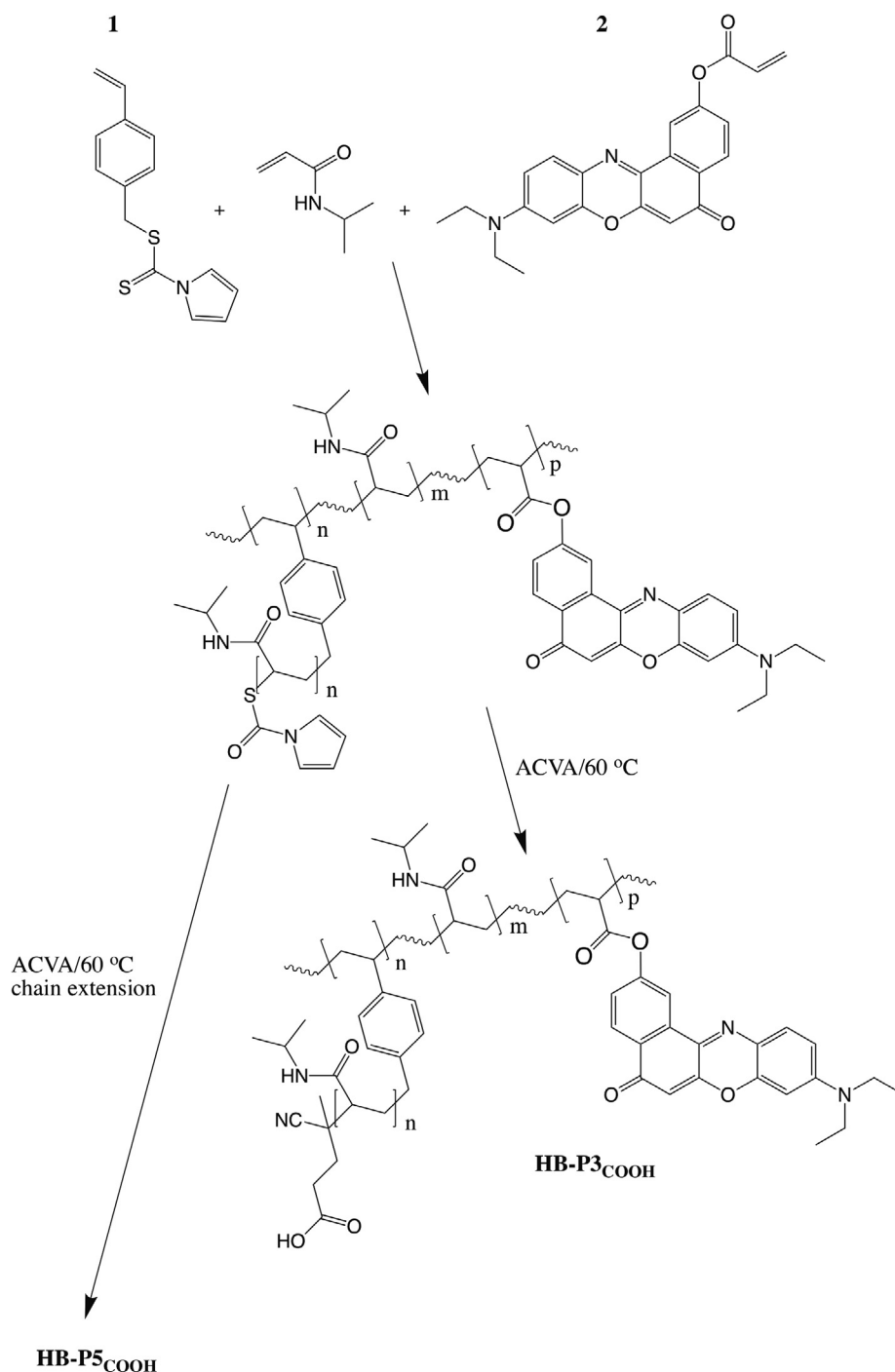
Scheme 1. 4-vinylbenzyl pyrrolecarbodithioate (**1**) based SCVP RAFT polymerisation of *N*-isopropyl acrylamide used to generate a HB-PNIPAM labelled Nile red (**2**) with post polymerization modification of the end groups by radical-radical coupling (**HB-P3$_{COOH}$**). The Scheme also shows how **HB-P3$_p$** was chain extended to provide a polymer with Nile red located in the inner core (**HB-P5**). **HB-P6** and **P7** were created in a similar manner by chain extending, with monomer mixtures containing **2**, a core polymer (**HB-P4**) without pendent Nile red (**P4**).

HB-P4$_p$ was prepared in the same manner as **HB-P3p** but without the inclusion of **2**. **HB-P6p** and **HB-P7p** polymers were produced by a stepwise chain extension of **HB-P4p** with NIPAM, **1** and **2** or NIPAM and **2**, respectively. The end groups of **HB-P3p**, **HB-P5p**, **HB-P6p** and **HB-P7p** were modified to carboxylic acid followed by addition of vancomycin, via the NHS ester, as previously described [1]. Characterisation of these polymers is provided in supporting information.

2.2. Polymer characterisation

Size exclusion chromatography (SEC), carried out in methanol, was used to determine the molar mass distributions. Samples (concentration = 1 mg ml^{-1}) were eluted through two Agilent Polargel columns (high molar mass range) maintained at a constant 30 °C with a 1 ml min^{-1} flow rate. Chemical characterisations including ^{1}H NMR, FTIR and sulphur elemental analysis are described in
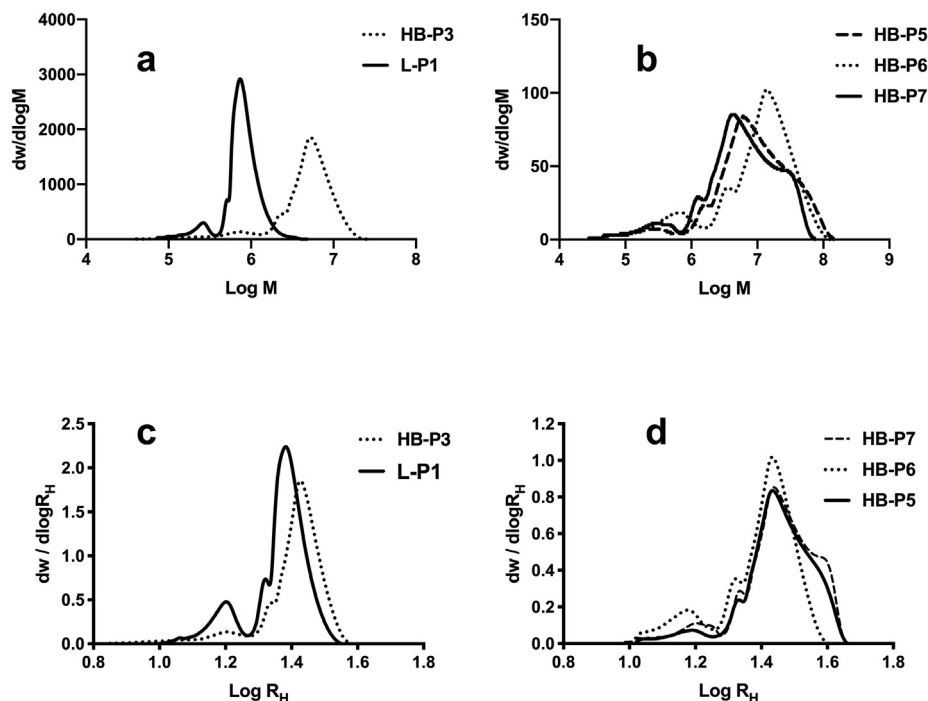
Fig. 2. Log molar mass distributions of one step (A) and chain extended (B) vancomycin-functional polymers and hydrodynamic radii distributions of one step (C) and chain extended (D) vancomycin-functional polymers.

the supporting information (Section 2). The temperature dependent nature of the polymers was studied via fluorescence emission, turbidimetry and microDSC measurements, which are also described in supporting information (Section 1.5). Peptide binding experiments of the polymers were carried out using a Vancomycin ELISA described in supporting information 1.5.3.

2.3. Microbiology studies

2.3.1. Bacterial strains

A reference strain of *Staphylococcus (S.) aureus* ('Oxford' NCTC 6571) and *S. epidermidis* were used as representative Grampositive bacteria, while *Pseudomonas (P.) aeruginosa* and *Escherichia (E.) coli* were used as a representative Gram-negative bacteria. The details of the cultures are included in supporting information.

2.3.2. Microbiological analysis

Polymer/Bacteria interactions were studied via fluorescence, confocal microscopy and agglutination (matt-button) assays, which are described in the supporting information (Section 1.6).

2.4. Statistical analysis

Fluorescence data of dilute solution polymer samples (Figs. 3 and 4) were recorded in triplicate, and the data fitted to a Gaussian distribution to determine fluorescence wavelength using GraphPad Prism 8.0.0. Significance was determined using goodness of fit with χ^2. Error bars are smaller than the data points shown on Figs. 3 and 4. The fluorescence of the samples of bacteria was recorded with n = 3, and the error bars are the standard error of the mean (Figs. 6 and 7). Quantitative fluorescence response to bacteria were compared by ANOVA and Fisher *post-hoc* analysis using Graphpad Prism 8.0.0 to determine the significance between samples.

3. Results and discussion

3.1. Materials

Molar mass distributions (SEC in methanol [19]) and functionalization loading of vancomycin polymers are shown in Table 1 and Fig. 2. The data from the precursor polymers and ^{1}H NMR, FTIR data are included in supporting data (Section 2). Both the
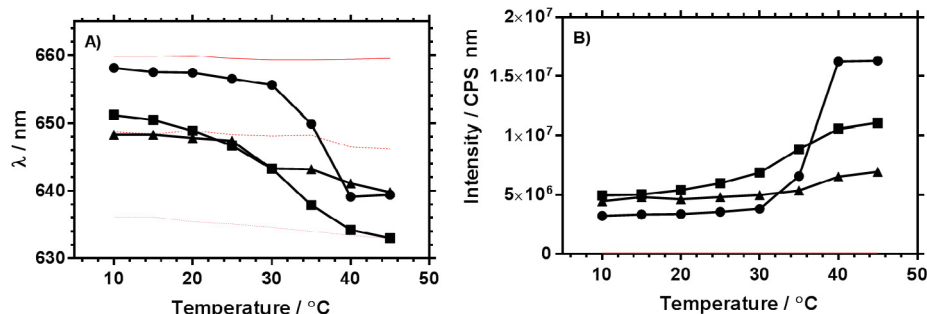

Fig. 3. Peak fluorescence emission wavelength (A) and integrated emission intensity (B) of linear polymers. (● **L-P0**, ■ L-P1$_{COOH}$ and ▲ L-P1) compared to water, ethylene glycol and methanol.
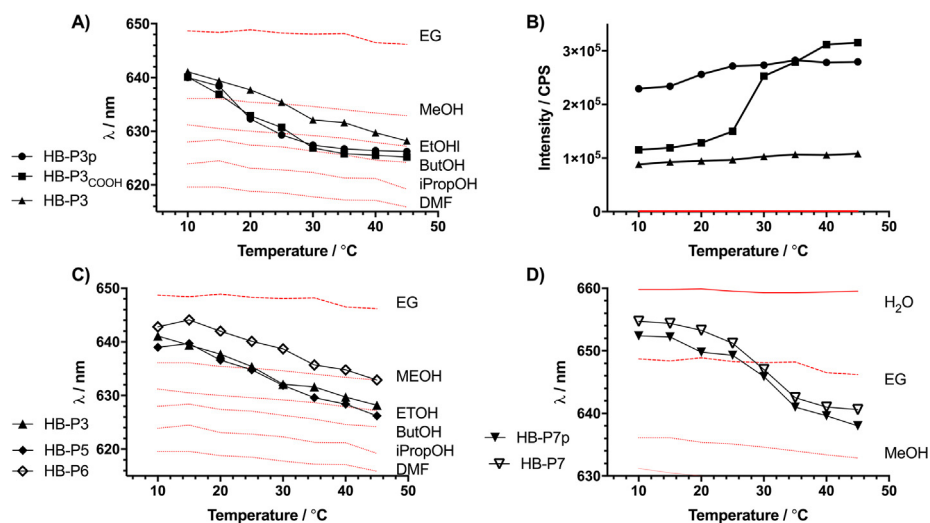
Fig. 4. Shift in peak fluorescence emission wavelength (A) and integrated emission intensity (B) with temperature of HB-PNIPAMs, with pyrrole (**HB-P3p**), acid (**HB-P3$_{COOH}$**) and vancomycin (**HB-P3**) chain ends. (C) Shift of fluorescence emission wavelength of **HB-P5**, **HB-P6** and **HB-**P3 with temperature. (D) Shift of fluorescence emission wavelength of **HB-P7$_p$** and **HB-P7** with temperature.

Table 1
Molar mass averages (kg mol^{-1}) from SEC analysis of linear and branched copolymers with vancomycin functionality.

	$\overline{M_n}$	$\overline{M_w}$	$\overline{M_z}$	α	M	Q_1	Q_3	DB[a]	van[b]
L-P1	554	661	810	0.51	588.8	204.2	4,786.3	0.043	0.133
L-P2	637	847	1,054	0.68	427.6	228.6	801.7	0.041	0.106
HB-P3	2,238	5,672	7,658	0.29	1,000.0	199.5	5,011.9	0.037	0.0617
HB-P5	1,897	16,415	40,657	0.42	2,398.8	309.0	19,054.6	0.050	0.0972
HB-P6	1,020	8,299	16,201	0.38	3,801.9	645.6	21,877.6	0.051	0.1341
HB-P7	1,471	10,575	23,633	0.34	3,801.9	199.5	21,877.6	0.084	0.0358

[a] Degree of Branching is ratio of benzyl groups: NIPAM from ^{1}H NMR. [b] loading of vancomycin (per mg polymer) as determined by ELISA.

Table 2
Medians and percentiles of the hydrodynamic radii.

Percentiles/nm	25%	50%	75%
HB-P1	11.0	17.3	26.3
HB-P2	14.5	19.6	26.1
HB-P3	14.3	21.3	30.9
HB-P5	15.7	23.1	32.9
HB-P6	15.0	21.2	29.4
HB-P7	14.7	22.7	32.4

Table 3
T$_{c-g}$ (°C, μDSC) of Linear PNIPAM and HB-PNIPAM polymer with varying functionality. **L-P1,$_{COOH}$** and **HB-P3,$_{COOH}$** are **L-P1** and **HB-P3** with carboxylic acid chain functional groups.

Polymer	T$_{c-g}$/°C	
	Linear	HB-PNIPAM
Unmodified (Polymer-NR)	33.0 (**L-Po**)	19.2 (**HB-P3P**)
Acid derivative (Polymer-COOH)	34.0 (**L-P1,$_{COOH}$**)	22.2 (**HB-P3,$_{COOH}$**)
Vanc. derivative (Polymer-van)	36.0 (**L-P1**)	32.0 (**HB-P3**)

Table 4
Fluorescence peaks (wavelength, λ and intensity, I) of linear PNIPAM polymers in dilute solution from 10 to 45 °C, in deionized water.

Polymer	10 °C λ$_{em}$/nm	45 °C λ$_{em}$/nm	10 °C I/10^3 CPS	45 °C I/10^3 CPS
L-P0	658	639	136	300
L-P1$_{COOH}$	651	633	146	223
L-P1	648	639	121	160

conventional molar mass averages and also the centile data are provided in Table 1. In our approach we consider that describing the molar mass distribution using the centiles may be more appropriate for these complex and non-gaussian molar mass distributions. As expected the values of the Mark-Houwink-Sakurada exponent, α, for the branched polymers were lower (α < 0.5) than those observed for the linear polymers. Flexible linear polymers cannot attain α < 0.5 in solution so that this indicates architecture other than linear; i.e. branched. The SEC method provides the distributions of the hydrodynamic radii (R$_H$) and these are also shown in Fig. 2. Table 2 provides the centiles of these data. Fig. 2C shows that it was possible to produce a linear polymer and a highly branched polymer with similar distributions of R$_H$ and Fig. 2D shows that the segmented branched polymers with Nile red situated in either inner domains (**HB-P5**), branched outer (**HB-P6**) or linear outer (**HB-P7**) had similar distributions of R$_H$.

Estimates of the peak temperature of the T$_{c-g}$ that are not dependent on aggregation behaviour can be obtained using calorimetry (Table 3) [12,20–22]. The data show that at each stage of the modification the branched polymers had T$_{c-g}$s that were lower than the similar linear polymers. Cloud point data from turbidimetry are also included in the supporting data (Section 2.6).

3.2. Thermally induced conformational response of polymers produced in one step synthesis

To examine the effect of the coil-to-globule transition on Nile red attached to linear PNIPAM a linear copolymer of NIPAM and **2** was prepared (**L-P0**). A dilute solution of **L-P0** was excited at 580 nm and the emission wavelength (λ$_{em}$) was observed to

Table 5
Fluorescence (wavelength, λ and integrated emission intensity, I) of HB-PNIPAMs polymer (**HB-P3$_p$**, **HB-P3$_{COOH}$** and **HB-P3**) in dilute solution from 10 to 45 °C.

Polymer	10 °C λ_{em}/nm	45 °C λ_e/nm	10 °C I/10^6 CPS	45 °C I/10^6 CPS
HB-P3$_p$	640	626	20.5	30.1
HB-P3$_{COOH}$	640	625	10.4	36.6
HB-P3	641	628	7.8	11.6

change as the sample was heated to 45 °C (Fig. 3). This shift in the fluorescence wavelength ($\Delta\lambda_{em}$ 19 nm) can be compared to the shift that Nile red undergoes in solvents of known relative polarity (illustrated in supporting data, Section 2.7). Also, shown in Fig. 3, an increase in integrated emission intensity (area under the emission peak) was observed as the label became shielded from quenching by the solvent [18] but the increase in intensity was much greater for **L-P0** (the linear polymer with COOH or vancomycin functionality) than in the other two materials. Comparison of the behaviour of the dye in the different solvents to its behaviour in the polymer allowed us to suggest how the microenvironment of the dye and the attached polymer segment changed across the T$_{c-g}$. Fig. 4 shows that in the open coil solvated conformation the tethered Nile red behaves in a similar manner to the dye dissolved in water [18], although tethering to the chain decreased λ_{em} below the T$_{c-g}$ and this indicated that the dye was in a less solvated environment than in water. Above the T$_{c-g}$ the polymer became desolvated and this resulted in a shift in λ_{em} to a value that was above that observed in the less polar species, ethylene glycol (relative polarity (RP) = 0.790) but less than methanol (RP = 0.762) [23]. Therefore, the data showed that the desolvated state of this linear polymer could be approximated to an environment in which 0.76 < RP < 0.79.

The $\Delta\lambda_{em}$ of the **L-P1$_{COOH}$** (651 to 632 nm, 1.00 < RP < 0.79 to RP $\approx$ 0.76) at the T$_{c-g}$ was greater than $\Delta\lambda_{em}$ when the repeat units of **3** were modified with vancomycin (**L-P1**) ($\Delta\lambda_{em}$, = 9 nm after modification with vancomycin). The reduction in the $\Delta\lambda_{em}$ reflects a smaller change at the T$_{c-g}$. The data suggested that in the linear polymers the presence of vancomycin increased the degree of swelling of the globular state as this charged unit increased the osmotic potential within the globule.

The highly-branched polymers (**HB-P3$_p$, HB-P3$_{COOH}$** and **HB-P3**) with Nile red throughout the chain were examined using the same methodology as the linear polymers. The polymers showed both shifts in λ_{em} and increases in fluorescence intensity (Fig. 4, Table 5, see electronic supporting information, Section 2.7, for full dataset). It is evident that the peak emission wavelength of the highly branched polymer changed over the studied temperature range with decreasing λ_{em} as the swollen (below T$_{c-g}$) polymer became desolvated.

The HB-PNIPAM with pyrrole end groups (**HB-P3$_p$**) displayed a clear step change in the λ_{em} at 15 °C. However, HB-PNIPAM with vancomycin end groups (**HB-P3**) showed a much more gradual decrease in λ_{em} across a larger temperature range. Although modification of the polymer with the vancomycin does not affect the initial or end polarity of the copolymerized dye (below T$_{c-g}$

Table 6
T$_{c-g}$ (°C) of HB-PNIPAM polymers with varying end groups determined by Micro DSC.

| Polymer | End groups | | |
	Pyrrole	Acid	Vancomycin
HB-P5	21.0	23.6	31.0
HB-P6	21.0	24.2	33.4
HB-P7	29.2	29.3	33.0

0.79 < RP < 0.76, above T$_{c-g}$ 0.76 < RP < 0.58) it both raised and broadened the T$_{c-g}$, removing the step change in behaviour seen with the linear polymer.

Below the T$_{c-g}$, Tables 3–5 and Figs. 3 and 4 show that highly-branched polymers had a lower λ_{em} (and therefore lower relative polarity) than the linear polymers. Although the linear **L-P1$_{COOH}$** copolymer demonstrated that inclusion of hydrophobic aryl units does lower the peak emission wavelength of the Nile red below that of the **L-P0** polymer, λ_{em} is still far higher than in the branched structure. Additionally, in the linear polymer vancomycin functionalization reduced the response of the fluorophore at the T$_{c-g}$. On the other hand, the magnitude of the shift in λ_{em} (between 10 and 45 °C) was maintained when the end groups of the branched polymer were modified with vancomycin.

3.3. Thermally induced conformational response of segmented polymers produced by two step synthesis

The polymers with extended chains containing Nile red in different segments were compared to the polymers containing Nile red throughout the polymer. In these systems the Nile red can be positioned in either the polymer core or the outer segments. Control of the placement of Nile red can potentially provide information on the behaviour of different segments as well as providing a route to optimising the change in fluorescence obtained as the polymer passed through the phase transition. The peak temperatures of the phase transitions were determined and are shown in Table 6 and the cloud points are provided in supporting information (Section 2.6). A clear distinction can be made between the polymers with different architecture in the second block, the branched-branched polymers (**HB-P5** and **HB-P6**) had a much lower T$_{c-g}$ than the branched-linear equivalents (**HB-P7**).

The polymers with extended chains containing Nile red in different segments (either inner or outer) were compared to the polymers containing Nile red throughout the polymer. Control of the placement of Nile red can potentially provide information on the behaviour of different segments as well as providing a route to optimising the change in fluorescence obtained as the polymer passed through the phase transition. The peak temperatures of the phase transitions were determined and are shown in Table 6. A clear distinction can be made between the polymers with different architecture in the second block, the branched-branched polymers (**HB-P5** and **HB-P6**) having a much lower T$_{c-g}$ than the branched-linear equivalents (**HB-P7**).

We considered that the outer segments of the branched polymers could be more swollen than the inner segments as the end groups partially penetrated the outer regions. If this is the case Nile red added to the outer block of the polymers potentially exists in a more polar environment compared to its placement throughout the polymer or within the inner block of the polymer chain.

Fig. 4 provides evidence to support this hypothesis. The figure compares the λ_{em} obtained from the polymers with Nile red positioned throughout the polymer (**HB-P3**), in the inner segments (**HB-P5**) or in the outer segments (**HB-P6**).

The data showed that λ_{em}, as proposed, was lower in **HB-P3** and **HB-P5** materials (above T$_{c-g}$ 0.76 < RP < 0.58) than in the **HB-P6** material (RP above the T$_{c-g}$ $\approx$ 0.76). HB-PNIPAM, **HB-P4$_p$**, was chain-extended by copolymerization of NIPAM and **2** in the absence of additional branching monomer to produce a labelled linear outer shell, **HB-P7$_p$**. Then this was modified to produce **HB-P7**, with vancomycin end groups. Fig. 4D shows that both of these polymers (**HB-P7$_p$** and **HB-P7**) provided a step change in $\Delta\lambda_{em}$ on heating; λ_{em} increased at 10 °C from 640 to 655 nm (below T$_{c-g}$ 1.00 > RP > 0.79, above T$_{c-g}$ 0.69 < RP < 0.76).

Importantly, the presence of the Nile red in a linear portion of the highly branched system resulted in a step change compared
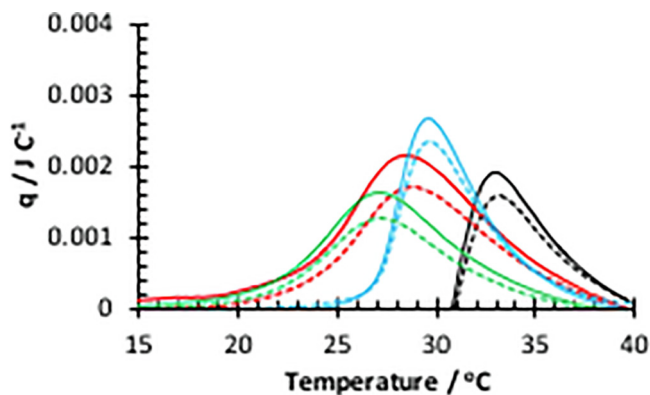
Fig. 5. Micro-DSC curves for HB-PNIPAM in absence (solid lines) and presence (dashed lines) of D-Ala-D-Ala peptide in PBS. Linear polymer (**L-P1**) (black), **HB-P3** (red), **HB-P6** (green) and **HB-P7** (blue).

to the more gradual reduction in λ_{em} observed in highly branched systems. Also, the step change in λ_{em} occurred within a similar temperature range as the phase transition observed by calorimetry reported in Table 6.

3.4. Peptide interactions of vancomycin derivatized polymers

Ala-ala is the *in vivo* target [24–28] for vancomycin and the binding response of vancomycin-functionalized polymers with bacteria can be at least partially replicated by studying their interaction with low concentrations of this dipeptide. There are assumptions made in these experiments around its use in that by binding to this peptide in isolation from the peptido glycan we ignore any effects of the rest of macromolecule and its location on the bacteria.

Changes in the state of solvation on binding can be inferred, using differential scanning calorimetry (DSC), by considering that binding either shifts the T_{c-g} or the total amount of water involved in the transition changes. Secondly, the location of the Nile red groups allowed us to use fluorescence spectroscopy to examine the behaviour of different domains within the polymer. Studies with the peptide and bacteria were carried out in PBS as a solvent as opposed to water as there are significant ion effects on the solubility of these stimuli-responsive macromolecules [4]. When the samples were dissolved in PBS the branched vancomycin polymers exhibited a cloud point that was not observed in water see supporting information, Section 2.6).

Calorimetry of the thermal collapse of the polymers showed that the interaction between the polymers and the peptide is more complicated than simply lowering the T_{c-g} (Fig. 5). Polymers dissolved in PBS (5 mg ml^{-1}) underwent an enthalpic transition accompanying the desolvation from the solute but the process of binding did not lower the peak temperature substantially. However, the magnitude of the peak diminished on binding and this

indicated that smaller amounts of water were involved in the transition. The decrease is quantified in Table 7.

In each case the enthalpy of the transition was decreased after the addition of the N-acetyl-D-Ala-D-Ala peptide. Further experiments showed that increasing the concentration of N-acetyl-D-Ala-D-Ala peptide did not further decrease the enthalpy of the coil-to-globule transition. The concentration of peptide (100 µg) was set in excess of the amount of vancomycin present in all the polymer systems as determined via the ELISA assay.

Solutions of polymer and peptide were produced and the fluorescence spectra of these systems were measured for 30 min following mixing at various temperatures. Little change in fluorescence wavelength was observed for these systems but an increase in peak maximum intensity was observed following mixing (Table 8, full details are available in electronic supporting information, Section 2.7). The linear polymer (**L-P1**) showed a significant increase in integrated emission intensity compared to the sample in the absence of peptide after mixing at 35 °C, whereas these samples at lower temperature showed little increase (<10^4 CPS nm) in integrated emission intensity after addition of the peptide. The branched polymer with Nile red located in the core (**HB-P5**) shows no response to peptide binding, with no more than 10^4 change in either direction upon binding. These data provided evidence that segmental collapse does not affect the polymer core.

Comparatively polymers with Nile red only in the outer extended segments (**HB-P6** and **HB-P7**) showed substantial increase in fluorescence intensity at 35 °C. These responses are large and occur within ten minutes. The responses were similar to those observed with the **HB-P3** polymer.

3.5. Interactions of bacteria with vancomycin functionalised polymers

The integrated emission intensity, 5 min after mixing, of Nile red contained in polymers **L-P1** and **HB-P3** was measured at 35 °C in the presence of varying concentrations of Gram-positive (*S. aureus, S. epidermis*) and Gram-negative (*E. coli*) bacteria (Fig. 6). Fig. 6A shows that both of the Gram-positive bacteria were added to the highly branched polymer (**HB-P3**) provided a marked increase in integrated emission intensity that was observed even at low concentration of bacteria (colony forming units; cfu per mass of polymer; 10^{-3} cfu µg^{-1}). The data showed a strong correlation between integrated emission intensity and the reduced concentration of bacteria (**HB-P3** slope 0.0219, R^2 0.912 and **L-P1** slope 0.0017, R^2 0.918).

This branched polymer provided a clear increase in fluorescence at 10^{-3} cfu µg^{-1} of polymer but only a slight increase in fluorescence and at much higher concentrations of bacteria (above 10^3 cfu µg^{-1} of polymer) was observed with the equivalent linear polymer (**L-P1**), as shown in Fig. 6B. The response to bacteria was almost immediate.

E. Coli is a Gram-negative species and the data in both Fig. 6A and B showed that there was no significant increase in fluorescence on mixing this species with either polymer. In supporting information (Section 2.8) the data have been reprocessed to show

Table 7
Peak T_{c-g} and heat release of vancomycin functional PNIPAM polymers in PBS with and without N-acetyl-D-Ala-D-Ala peptide.[a]

Polymer	Free		Bound		
	T/°C	q/mJ	T/°C	q/mJ	Δq/mJ
L-P1	33.9	8.7	34.1	7.3	1.4
HB-P3	29.0	19.8	29.3	14.4	5.4
HB-P6	27.5	13.9	27.5	9.9	4.0
HB-P7	30.3	15.9	30.3	12.4	3.5

[a] Fixed concentration of 100 µg D-Ala-D-Ala peptide.

Table 8
Change in integrated emission intensity ($\Delta I/10^3$ CPS) and time taken to reach peak intensity (T/minutes) of vancomycin derivatized PNIPAM polymers on binding of D-Ala-D-Ala Peptide at different temperatures.

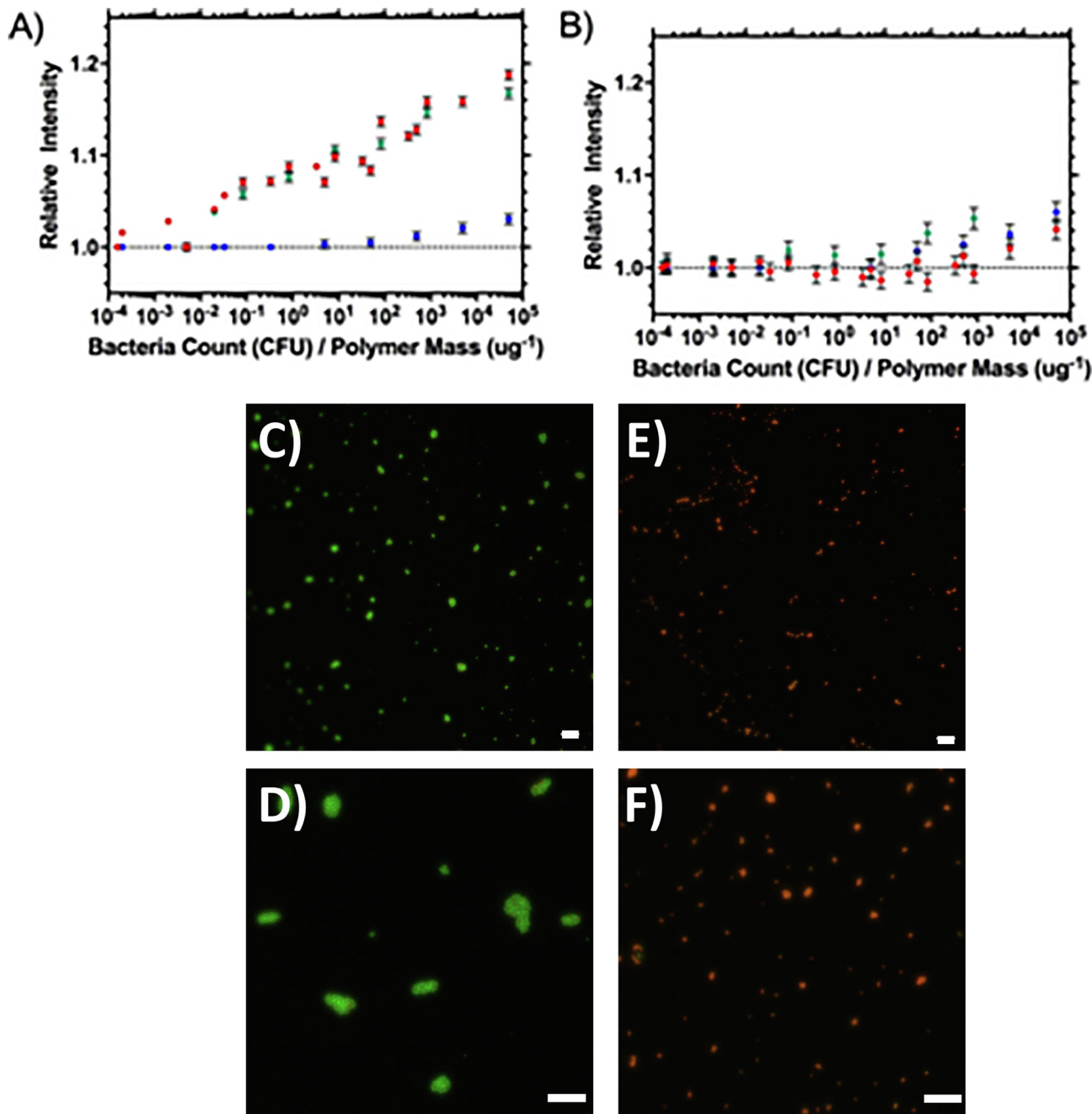| ΔI (10^3 CPS nm)/T (minutes)				
Polymer	10 °C	15 °C	25 °C	35 °C
L-P1	**5**/0	**0**/–	**0**/–	**23**/5
HB-P3	**50**/5	**35**/0	**10**/5	**80**/5
HB-P5	**0**/–	−5/–	**10**/0	**10**/0
HB-P6	**15**/0	**10**/0	−5/0	**50**/5
HB-P7	**20**/0	**25**/0	−10/0	**50**/10

Fig. 6. Relative fluorescence integrated intensity of (A) **HB-P3** and (B) **L-P1** mixed with Gram-positive and negative colonies of bacteria (♦ *S. aureus*, ♦ *S. epidermis* and ♦ *E. coli*), measured 5 min after mixing at 35 °C. Error bars are standard error of the mean. (C) to (F); Micrographs stained using live/dead stain®. (C) shows live (green) S, aureus and (E) shows the bacteria after being killed by exposure to *iso*propanol. (D) is an example of a micrograph of live bacteria after aggregation with **HB-P3** and (F) shows the result of adding **HB-P3** to dead bacteria. The data show that there was little or no aggregation when **HB-P3** was exposed to dead bacteria but extensive aggregation with live bacteria.
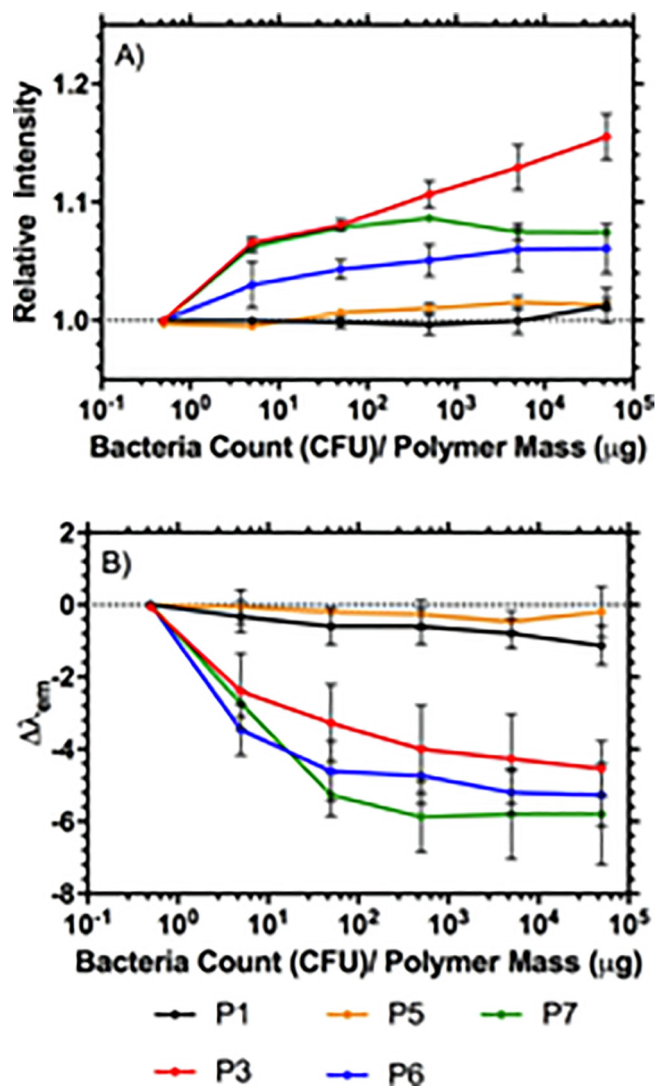
Fig. 7. (A) Relative Fluorescence Integrated Intensity and (B) Wavelength shift of PNIPAM-van polymers (**L-P1**, **HB-P3**, **HB-P5**, **HB-P6**, **HB-P7**) exposed to increasing amounts of *S. aureus* relative to amount of polymer, measured 5 min post mixing at 35 °C. Error bars are standard error of the mean.

the effect of adding increasing concentrations of bacteria at constant polymer concentration. Treatment of the data in this way allowed us to show that for *S. aureus* and *S. epidermis* an increase in fluorescence intensity can be observed with as little as 10 CFU mL^{-1} of bacteria. The procedure was repeated at 15 °C and no increase in fluorescence was observed for either linear (**L-P1**) or branched (**HB-P3**) polymer.

Also, included in Fig. 6 are confocal microscopy images of both live and dead *S. aureus* with and without **P3**. The images show that only live bacteria were aggregated by **P3**. Dead bacteria also provided no shift in peak emission wavelength or intensity. These and further data including images of the bacteria/polymer aggregates are provided in supporting information (Section 2.8).

This temperature dependence confirmed previous work in this area [1] and is reflected in the temperature dependence of the desolvation on binding D-Ala-D-Ala that was reported in Table 8. In this previous work *S. aureus* bound to vancomycin-functional HB-PNIPAM at 37 °C but was released at 4 °C [1]. This study was followed further using only Gram-positive bacteria (*S. aureus*) at varying amounts of bacteria and the other branched polymers (Fig. 7). The linear polymer functionalised with pendant vancomycin

groups and Nile red (**L-P1**) showed neither an increase in the fluorescence intensity nor a shift in the emission peak wavelength. Similarly, there was no change in these properties when the polymer labelled in the inner segment (**HB-P5**) was put into contact with increasing amounts of bacteria. However, the analogous polymer with a labelled branched outer shell (**HB-P6**) did show an increase in fluorescence intensity and the emission peak wavelength shifted by 5 nm. Also, the polymer with a linear labelled outer shell (**HB-P7**) provided an increase in fluorescence intensity and a change in emission wavelength. In the intensity data sets (Fig. 7A) there were clear and significant differences between the behaviour of the **L-P1**, **HB-P5** group of polymers and the **L-P3**, **HB-P6**, **HB-P7** group of polymers ($p < 0.05$, ANOVA and Fisher's *post hoc* analysis) at all amounts of bacteria equal to and greater than 5 CFU μg^{-1} of polymer.

HB-PNIPAM with vancomycin end groups and with Nile red covalently attached provided a fluorescence signal of the presence of live bacteria.

4. Discussion

We have shown previously that HB-PNIPAM with vancomycin end groups binds to Gram-positive bacteria and then desolvates to form bacteria/polymer aggregates.[1] We also showed that analogous linear polymers do not behave in this way.[16] In this work we have further confirmed this behaviour and by using solvatochromic dyes in molecular design that placed dyes in different segments it was shown that Nile red situated either throughout the chain segments or localized in the inner or outer domains of the coils gave different responses to the binding of the D-Ala-D-Ala peptide or Gram -positive bacteria. These data were also compared to similar experiments with linear analogues and a HB-PNIPAM with chain extended linear end segments. Materials without the attached dye that do not provide a quantifiable fluorescence signal but do bind and aggregate bacteria in complex in vitro skin models were reported by us already [29]. The segments in the outer regions were in more polar environments than the inner regions even above the main T_{c-g}. The extent of desolvation on binding was larger for the branched (**HB-P3**) compared to the linear polymer (**HB-P1**); Δq is larger. The differences in the responses of Nile red after binding the vancomycin moieties to D-Ala-D-Ala were also dependent on architecture with larger changes in integrated intensity (ΔI) at all temperatures observed in the branched compared to the linear polymer. From the calorimetry data, at 35 °C, **HB-P3** had almost passed through the T_{c-g} and the fluorescence data indicated that on binding D-Ala-D-Ala a further desolvation occurred that was indicated by the large value of ΔI reported in Table 8 at this temperature. When examining the branched segmented polymers it was notable that there was little change in the peak emission wavelength nor the fluorescence intensity when Nile red was located in the inner segments of the polymer. These data showed that binding at the chain ends did not affect the solvation of the inner segments. On the other hand binding of the peptide had a large effect on the polymers with Nile red in the outer segments.

The branched polymers bound to *S. aureus* and the fluorescence intensity increased as the concentration of bacteria increased but there was essentially no increase in fluorescence intensity when the linear polymer or the polymer with Nile red in the inner segments was used. However, although the calorimetric and fluorescence experiments showed that binding of the D-Ala-D-Ala peptide induced a segmental desolvation both above and below the T_{c-g}, the correlation between increasing concentrations of bacteria and increasing fluorescence intensity was observed only above the main T_{c-g}, as the outer chain segments became desolvated.

5. Conclusion

This paper has shown that a solvatochromic dye can be incorporated into a highly-branched polymer such that it responded to binding of bacteria or the target peptide (for vancomycin). These polymers can be used to detect bacteria in a concentration dependent manner. Chain segments adjacent to ligands at the ends of a highly branched polymer desolvate on binding. On the other hand dyes located within the core of similar highly branched polymers or analogous linear polymers do not indicate changes in the environments of the relevant chain segments. The many applications of these systems in both the clinic and the environment are currently being studied.

6. Funding sources

Appendix A. Supplementary material

Supplementary data to this article can be found online at https://doi.org/10.1016/j.actbio.2019.01.066.

References

[1] J. Shepherd, P. Sarker, K. Swindells, I. Douglas, S. MacNeil, L. Swanson, S. Rimmer, Binding bacteria to highly branched poly(N-isopropyl acrylamide) modified with vancomycin induces the coil-to-globule transition, J. Am. Chem. Soc. 132 (6) (2010) 1736–1737.

[2] P. Sarker, J. Shepherd, K. Swindells, I. Douglas, S. MacNeil, L. Swanson, S. Rimmer, Highly branched polymers with polymyxin end groups responsive to Pseudomonas aeruginosa, Biomacromolecules 12 (1) (2011) 1–5.

[3] R.A. Plenderleith, C.J. Pateman, C. Rodenburg, J.W. Haycock, F. Claeyssens, C. Sammon, S. Rimmer, Arginine-glycine-aspartic acid functional branched semi-interpenetrating hydrogels, Soft Matter 11 (38) (2015) 7567–7578.

[4] Y. Zhang, S. Furyk, D.E. Bergbreiter, P.S. Cremer, Specific ion effects on the water solubility of macromolecules: PNIPAM and the hofmeister series, J. Am. Chem. Soc. 127 (41) (2005) 14505–14510.

[5] K. Sakota, D. Tabata, H. Sekiya, Macromolecular crowding modifies the impact of specific hofmeister ions on the coil-globule transition of PNIPAM, J. Phys. Chem. B 119 (32) (2015) 10334–10340.

[6] M.C.M. Costa, S.M.C. Silva, F.E. Antunes, Adjusting the low critical solution temperature of poly(N-isopropyl acrylamide) solutions by salts, ionic surfactants and solvents: A rheological study, J. Mol. Liquids 210, Part A (2015) 113–118.

[7] R. Liu, M. Fraylich, B. Saunders, Thermoresponsive copolymers: from fundamental studies to applications, Colloid Polym. Sci. 287 (6) (2009) 627–643.

[8] X. Zhu, C. Yan, F.M. Winnik, D. Leckband, End-grafted low-molecular-weight PNIPAM does not collapse above the LCST†, Langmuir 23 (1) (2007) 162–169.

[9] X.-P. Qiu, F. Tanaka, F.M. Winnik, Temperature-induced phase transition of well-defined cyclic poly(N-isopropylacrylamide)s in aqueous solution, Macromolecules 40 (20) (2007) 7069–7071.

[10] D. Magerl, M. Philipp, X.-P. Qiu, F.M. Winnik, P. Müller-Buschbaum, Swelling and thermoresponsive behavior of linear versus cyclic poly(N-isopropylacrylamide) thin films, Macromolecules 48 (9) (2015) 3104–3111.

[11] S. Carter, B. Hunt, S. Rimmer, Highly branched poly(N-isopropylacrylamide)s with imidazole end groups prepared by radical polymerization in the presence of a styryl monomer containing a dithioester group, Macromolecules 38 (11) (2005) 4595–4603.

[12] Y. Satokawa, T. Shikata, F. Tanaka, X.-P. Qiu, F.M. Winnik, Hydration and dynamic behavior of a cyclic poly(N-isopropylacrylamide) in aqueous solution: effects of the polymer chain topology, Macromolecules 42 (4) (2009) 1400–1403.

[13] L. Swanson, S. Rimmer, S. MacNeil, I. Douglas, K. Swindells, P. Sarker, Fluorescence resonance energy transfer confirms the bacterial-induced conformational transition in highly-branched poly(N-isopropyl acrylamide with vancomycin end groups on binding to Staphylococcus aureus, Soft Matter 10 (2014) 5824–5835.

[14] M.A. Cooper, M.T. Fiorini, C. Abell, D.H. Williams, Binding of vancomycin group antibiotics to d-alanine and d-lactate presenting self-assembled monolayers, Bioorg. Med. Chem. 8 (11) (2000) 2609–2616.

[15] Y. Gilbert, M. Deghorain, L. Wang, B. Xu, P.D. Pollheimer, H.J. Gruber, J. Errington, B. Hallet, X. Haulot, C. Verbelen, P. Hols, Y.F. Dufrêne, Single-molecule force spectroscopy and imaging of the vancomycin/d-Ala-d-Ala interaction, Nano Lett. 7 (3) (2007) 796–801.

[16] P. Teratanatorn, R. Hoskins, T. Swift, C.W.I. Douglas, J. Shepherd, S. Rimmer, Binding of bacteria to poly(N-isopropylacrylamide) modified with vancomycin: comparison of behavior of linear and highly branched polymers, Biomacromolecules 18 (9) (2017) 2887–2899.

[17] S. Chen, Q. Chen, Q. Li, J. An, P. Sun, J. Ma, H. Gao, Biodegradable synthetic antimicrobial with aggregation-induced emissive luminogens for temporal antibacterial activity and facile bacteria detection, Chem. Mater. 30 (5) (2018) 1782–1790.

[18] R. Plenderleith, T. Swift, S. Rimmer, Highly-branched poly(N-isopropyl acrylamide)s with core-shell morphology below the lower critical solution temperature, RSC Adv. 4 (92) (2014) 50932–50937.

[19] T. Swift, R. Hoskins, R. Telford, R. Plenderleith, D. Pownall, S. Rimmer, Analysis using size exclusion chromatography of poly(N-isopropyl acrylamide) using methanol as an eluent, J. Chromatogr. A 1508 (2017) 16–23.

[20] T. Principi, C.C.E. Goh, R.C.W. Liu, F.M. Winnik, Solution properties of hydrophobically modified copolymers of N-isopropylacrylamide and N-glycine acrylamide: a study by microcalorimetry and fluorescence spectroscopy, Macromolecules 33 (8) (2000) 2958–2966.

[21] C. Diab, Y. Akiyama, K. Kataoka, F.M. Winnik, Microcalorimetric study of the temperature-induced phase separation in aqueous solutions of poly(2-isopropyl-2-oxazolines), Macromolecules 37 (7) (2004) 2556–2562.

[22] S. Verbrugghe, A. Laukkanen, V. Aseyev, H. Tenhu, F.M. Winnik, F.E. Du Prez, Light scattering and microcalorimetry studies on aqueous solutions of thermo-responsive PVCL-g-PEO copolymers, Polymer 44 (22) (2003) 6807–6814.

[23] C. Reichardt, T. Welton, Solvents and Solvent Effects in Organic Chemistry, John Wiley & Sons, 2011.

[24] J.L. Carpenter, P. Camilleri, D. Dhanak, D. Goodall, A study of the binding of vancomycin to dipeptides using capillary electrophoresis, J. Chem. Soc., Chem. Commun. 11 (1992) 804–806.

[25] J. Eirich, R. Orth, S.A. Sieber, Unraveling the protein targets of vancomycin in living S. aureus and E. faecalis cells, J. Am. Chem. Soc. 133 (31) (2011) 12144–12153.

[26] S.J. Kim, L. Cegelski, M. Preobrazhenskaya, J. Schaefer, Structures of staphylococcus aureus cell-wall complexes with vancomycin, eremomycin, and chloroeremomycin derivatives by 13C{19F} and 15N{19F} rotational-echo double resonance†, Biochemistry 45 (16) (2006) 5235–5250.

[27] J.-G. Lee, C. Sagui, C. Roland, First principles investigation of vancomycin and teicoplanin binding to bacterial cell wall termini, J. Am. Chem. Soc. 126 (27) (2004) 8384–8385.

[28] M. Rekharsky, D. Hesek, M. Lee, S.O. Meroueh, Y. Inoue, S. Mobashery, Thermodynamics of interactions of vancomycin and synthetic surrogates of bacterial cell wall, J. Am. Chem. Soc. 128 (24) (2006) 7736–7737.

[29] J. Shepherd, P. Sarker, S. Rimmer, L. Swanson, S. MacNeil, I. Douglas, Hyperbranched poly(NIPAM) polymers modified with antibiotics for the reduction of bacterial burden in infected human tissue engineered skin, Biomaterials 32 (1) (2011) 258–267.